

# Translocation of Cyclophosphamide by Using Multi-Walled Carbon Nanotubes Into Mammalian Cancer Cells

P. S. Uttekar, V. V. Chopade

P. E. Society's, Modern College of Pharmacy, Nigdi, Pune, Maharashtra, India

## ABSTRACT

The aim of the present work was to prepare cyclophosphamide loaded MWCNTs for target drug delivery of Cyclophosphamide (CP), an Anti-Cancer drug. Experimental designing was done by using the Ultrasonic probe sonicator, PCI Analytics DP-120 under continuous stirring. Translocation of cyclophosphamide was done on functionalized MWCNTs. Functionalization of MWCNTs was done by Acid Purification of pure MWCNTs & conjugation of FA-EDA with oxidized MWCNTs. The loaded MWCNTs were characterized for various parameters including the MTT assay, DSC, SEM, FTIR, Zeta Potential, NMR, Particle Size Analysis, XRD, Stability Study & poly dispersive Index. It is worth that the cyclophosphamide loaded MWCNTs showed better targeting action.

### Highlights:

Functionalization of MWCNTs.

Loading of CP with FA-EDA-MWCNTs

Characterization of Cyclophosphamide anchored CNTs for various parameters.

**Keywords:** Multiwall Carbon nanotubes (MWCNTs), cyclophosphamide, Functionalization of MWCNTs, Translocation.

## I. INTRODUCTION

Cancer ranks amongst the top three killers in modern society, next to heart and cerebrovascular diseases. In 2009, according to World Health Organization (WHO), approximately eight million people died from cancer worldwide. In 1991, Sumio Iijima identified a new structural form of this allotrope (The discovery of the third allotropic form of carbon fullerene), the cylindrical fullerene and named them as carbon nanotubes (CNTs) <sup>(1,45)</sup>. CNTs are graphene sheets rolled into a seamless cylinder that can be open ended or capped, having a high aspect ratio with diameters as small as 1 nm and a length of several micrometer<sup>2</sup>. Carbon nanotubes are allotropes of carbon with a cylindrical nano structure. Nanotubes have been constructed with length to diameter ratio of upto 132000000:1, significantly larger than for any other material. These cylindrical carbon molecules have unusual properties, which are essential for nano technology, electronics, optics & other fields of materials, science & technology.

Their name is derived from their long, hollow structure with the walls forms by 1-atom-thick sheets of carbon, called graphene. These sheets are rolled at specific &

discrete ("chiral") angles, & the combination of the rolling angle & radius decides the nanotubes properties; for example, whether the individual nanotube shell is a metal or semiconductor. Nanotubes are categorized as single-walled nanotubes (SWNTs) & multi-walled nanotubes (MWCNTs). Individual nanotubes naturally align themselves into "ropes" held together by Vander Waals forces.

Applied quantum chemistry, specifically, orbital hybridization best describe chemical bonding in nanotubes. The chemical of nanotubes is composed entirely of sp<sup>2</sup> bonds, similar to those of graphite. These bonds, which are stronger than the sp bonds found in alkanes, provide nanotubes with their unique strength.

Carbon atoms have 3 allotropic forms:

- ✓ Diamond-sp<sup>3</sup> hybridization
- ✓ Graphite-sp<sup>2</sup> hybridization
- ✓ Fullerenes-sp<sup>2</sup> hybridization

CP is widely used in cancer chemotherapy, mostly in combination with other anti-neoplastic agents, and as an immunosuppressant. CP belongs to the group of alkylating agents and is a pro drug that is activated via 4-hydroxylation by cytochrome P450s to generate

alkylating nitrogen mustards. The resultant mustards can alkylate DNA to form DNA-DNA cross-links, leading to inhibition of DNA synthesis and cell apoptosis (7).

With more than 10 million new cases every year, cancer is one of the most devastating diseases. Though the current treatments of cancer by surgery, radiation, and chemotherapy are successful in several cases; however, these curative methods are likely to kill healthy cells and cause toxicity to the patient 8, 13. Many patients who succumb to death due to cancer do not die as a result of the primary tumor, but because of the systematic effects of metastases on the other regions away from the original site. The main problem associated with the various chemotherapeutic agents is the lack of selectivity towards cancerous cells. This problem can be overcome by using CNTs as a Nano carrier for anticancer drug.

## II. MATERIALS AND METHODS

### 2.1. Materials.

2.2. Carbon nanotubes were procured from Applied Science innovations Pvt ltd, pune, Cyclophosphamide was procured from Emcure Pune, folic Acid, N-Hydroxisuccinimide, N,N'-Dicyclohexylcarbodiimide & Di-ter butyl di-carbonate (t-boc) were procured from Sisco Research Lab.Pvt.Ltd, Ethylene Diamine was supplied by Thermo Fisher Scientific India Pvt.Ltd, MTT Reagent from Sigma Aldrich, Mumbai & MCF -7 Cells from NCCS pune.

### 2.3. Functionalization of MWCNTs.

#### 2.3.1 Acid Purification of Pure MWCNTs:

Acid treatment will be used for removal of catalytic and amorphous impurities from the unpurified MWCNTs. Firstly, the unpurified MWCNTs (pristine MWCNTs) (500 mg) treating in a microwave oven at  $400 \pm 2^\circ\text{C}$  for 2 hr. The microwave treated MWCNTs (500 mg) will reflux with a 200 ml mixture of concentrated Nitric and Sulphuric acid ( $\text{HNO}_3$ :  $\text{H}_2\text{SO}_4$  :: 1:3 ratio) in a flat bottom flask (equipped with the reflux condenser and thermometer) with continuous magnetic stirring at  $120 \pm 5^\circ\text{C}$  for 24 hr, upon completion of reaction, the mixture was washed with cold distilled water to remove the residual acid and then ultra-

centrifuged (20,000 rpm for 15 min) until the supernatant of the mixture represent the pH=7 which exhibit the no acidity in the suspension. The sample was then dried in a vacuum oven at  $80^\circ\text{C}$  for 4 h [19,20]

### 2.3.2 Conjugation of Folic Acid-Ethylenediamine with Oxidized MWCNTs (FA-EDA-MWCNTs):

#### Step I: Preparation of FA-NHS Ester

Folic acid (FA) (1 gm) was dissolved in dimethyl sulfoxide (40 ml) and triethylamine (0.5 ml) in a reaction vessel. Then, N-Hydroxy Succinimide (NHS) (520 mg) and Di-Cyclohexyl Carbodimide (500 mg) was added with continuous magnetic stirring at room temperature in dark for 18 hr. The mixture was filtered to remove precipitated side product dicyclohexyl urea, triethyl amine (TEA) was removed by evaporation under reduced pressure and remaining product was stored at  $-20^\circ\text{C}$ . The collected product was characterized by FTIR spectroscopy. [21]

#### Step II: Conjugation of FA-NHS Ester to Ethylene Diamine

The FA-NHS (150 mg) active ester was mixed with Ethylene diamine (75 ml) in DMSO (15 ml) in the presence of tri-ethyl amine (0.5 ml) with continuous magnetic stirring at 100 rpm for 24 hr at room temperature. The unconjugate ethylene diamine (EDA) was removed, filter, dry under vacuum to yield folate conjugate (FA-EDA-NH<sub>2</sub>) as a pale yellow solid and detect using UV visible spectrophotometer at  $\lambda_{\text{max}}$  363 nm. [21]

#### Step III : Conjugation of FA-EDA with Oxidized MWCNTs(FA-EDA-MWCNTs)

Oxidized MWCNTs (50 mg) will disperse in DMSO and N-ethyl-N'-(3-dimethyl-aminopropyl)Carbodimide hydrochloride (EDAC) dissolve in DMSO (6.41 mg/ml) was added to it with continuous magnetic stirring (100 rpm) for 6 hr, followed by addition of FA-EDA-NH<sub>2</sub> (4.60 mg/ml). The reaction was continue under vigorous stirring upto 5 days and remaining unconjugated FA-EDA-NH<sub>2</sub> was removed by dialysis, the product was collected, dried and characterized by FTIR spectroscopy. [20,21]

### 2.3.3 Loading of Cyclophosphamide molecule with CNTS (FA-EDA-MWCNTs/CP):<sup>[1]</sup>

Cyclophosphamide (30mg) in triethylamine (TEA) was mixed with FA-EDA-MWCNTs (10mg) dispersion in phosphate buffer solution (PBS; pH 7.4) with continuous magnetic stirring upto 48 h at room temperature in dark condition.

## III. CHARACTERISATION OF CYCLOPHOSPHAMIDE LOADED MWCNTS

### 3.1 FTIR SPECTROSCOPY:

Utilizing FTIR, functional groups that may be present on particle can be identified. The potassium bromide (KBr) disks with sample were prepared using electrically operated KBr Press Model HP-15. About 1 mg of sample was triturated with about 5 mg of dry KBr and then pressed into the disks. The FTIR spectrum was recorded using Jasco 4100 (TOKYO, JAPAN) with IR resolution software. The scanning range was 4000-400  $\text{cm}^{-1}$ .

### 3.2 U.V. VISIBLE SPECTROSCOPY:

The U.V. Spectroscopy studied by using U.V. Visible Spectrophotometer (Jasco V630).

The U.V. visible spectrum of pure Cyclophosphamide, Amide F-MWCNTs, Cyclophosphamide loaded to MWCNTs and unbound cyclophosphamide molecules were obtained in water as a solvent. Samples were scanned over the range of 200-400 nm by using U.V. Visible Spectrophotometer (Jasco V630) and observe the various peak obtained.

### 3.3 N.M.R SPECTROSCOPY:

The proton magnetic resonance spectrometry has been extensively used as a fundamental tool for the determination of structure of the synthesized compounds.

The  $^1\text{H}$  NMR spectra of the synthesized compounds such as Oxidised MWCNTs, Amide Functionalized MWCNTs and Loaded Cyclophosphamide on F-MWCNTs were recorded in DMSO (unless specified) with TMS as internal reference (chemical shift in  $\delta$ , ppm) using MERCURY VARIAN 500 MHz instrument and MERCURY VARIAN 300 MHz instrument.

### 3.4 SCANNING ELECTRON MICROSCOPY (SEM):

The detailed surface characteristics of the pure Carbon Nanotubes and Carbon Nanotubes loaded on Cyclophosphamide were observed by using a JEOL Scanning Electron Microscope (Model: JSM 6360 A, Japan). SEM was the most commonly used method for characterizing particulate drug delivery system. SEM was used to determine surface topography, texture and to examine the morphology of fractured surface.

The samples were attached to the specimen holder to aluminium stab by using a double coated adhesive tape and gold coated (20 nm thickness) under vacuum using sputter coater (Model : IB-2, Hitachi, Tokyo, Japan) during gold coating process the samples were exposed to vacuum for 5-10 min at 40 mA and investigate a accelerating voltage of 15 kV and 10 kV was applied and the image was photographed by Asia Pentax Camera. Particle surfaces were evaluated at different magnification of 10X, 100X, 1000X and 3000X.<sup>[25]</sup>

### 3.5 P-X.R.D. SPECTROSCOPY:

Powder X-Ray Diffraction (P-XRD) measurement of pure Cyclophosphamide and cyclophosphamide loaded on functionalized Multi-Walled Carbon Nanotubes (MWCNTs) was performed by using Philips (PW 3710) Expert Pro MPD Diffractometer (PAN Analytical Inc, Germany) with resolution of 0.001  $\text{\AA}^\circ$ .

The sample of 10 mg was sprinkled on vacuum grease applied glass slide to make a layer having a thickness of 0.5 mm and slick the sample to slide before measurement. The samples were radiated using a Copper target tube. Scanning angles ranged from 5° to 60° of 2 $\theta$ . The current used was 40 mA and voltage 40 kv.<sup>[27]</sup>

### 3.6 DIFFERENTIAL SCANNING CALORIMETRY (DSC):

Pure Cyclophosphamide and Cyclophosphamide loaded on Functionalized Multi-Walled Carbon Nanotubes (F-MWCNTs) was analysed for DSC analysis using Differential Scanning Calorimetry equipped with an intra-cooler (DSC METTLER STAR<sup>®</sup>SW 12.10, Switzerland).

The analysis was carried out on an approximately 2-5 mg of sample sealed in standard pierced aluminium pans (Al -Crucibles, 40 Al). An empty aluminium pan used as reference. An inert atmosphere was maintained by

purging nitrogen gas at a flow rate of 25 ml/min at a scanning rate of 10°C/min from 50°C to 300°C.

### 3.7 PARTICLE SIZE ANALYSIS:

The mean particle size of pure MWCNTs and Cyclophosphamide Loaded on F-MWCNTs were analysed by using (HORIBA Scientific, Nano Particle SZ-100 Series JAPAN) particle size analyzer.

Particle size analysis is performed by dynamic light scattering (DLS) at a scattering angle of 90° at 25 °C using appropriately diluted samples. Exactly 5 mg of pure MWCNTs and Cyclophosphamide loaded on F-MWCNTs were dispersed in 10 ml of deionized water, followed by sonication for 7 min and the resulting suspension was introduced into the measurement chamber. Each sample was measured in triplicate in the analysis. The particle size analysis is the important parameter because it influences the physicochemical properties & biological fate of the nanoparticles after in vivo administration.

### 3.8 POLY DISPERSITY INDEX (PDI):

It is also called as Heterogeneity index. It is a measure of the width of molecular weight distributions.

The PDI of pure MWCNTs and Cyclophosphamide Loaded on F-MWCNTs were analysed by using (HORIBA Scientific, Nano Particle SZ-100 Series JAPAN) particle size analyzer.

### 3.9 Zeta Potential:

Zeta potential is an important parameter to analyze the long-term stability. Zeta potential (ZP) refers to the surface charge of the particles. ZP ( $\pm$ ) indicates the degree of repulsion between close and similarly charged particles in the dispersion. This repulsion force prevents aggregation of the particles. Therefore, ZP is a useful parameter to predict the physical stability. Zeta potential is the most important parameter for physical stability of nanoparticles. The higher the electrostatic repulsion between the particles the greater is the stability. ZP value more than +20 mV or less than -20 mV predicts good physical stability of nanoparticle dispersion.

A sample of pure MWCNTs and Cyclophosphamide loaded on F-MWCNTs was extemporaneously diluted in Milli-Q (Millipore Corp., USA) water (1  $\mu$ l/10 ml) and injected in to the apparatus. The measurements were

carried out in the fully automatic mode. Each sample was measured in triplicate in the analysis.

### 3.10 In-vitro release studies:

The dispersion of FA-EDA-MWCNTs/CP of conjugates were studied in sodium acetate buffer (pH 5.3) and phosphate buffer (pH 7.4) as recipient media using a dissolution method maintaining 37 $\pm$ 0.5°C physiological temperature. The MWCNTs conjugates were filled in pre-treated dialysis membrane separately and kept into the releasing media under magnetic stirring at 37 $\pm$ 0.5°C. At definite time points, the MWCNTs samples were withdrawn and after each sampling the withdrawn medium was replenished with fresh sink solution maintaining strict sink condition. The drug concentration was determined by UV Visible spectrophotometer. <sup>[6]</sup>

### 3.11 EX-VIVO STUDY:- CELL CULTURE STUDY METHYL THIAZOLE TETRAZOLIUM (MTT) ASSAY (Cytotoxicity Assay/ Cell Viability Assay):

The MTT assay is a colorimetric assay for assessing cell metabolic activity. The NAD(P)H dependent cellular oxido-reductase enzymes may, under defined conditions, reflect the number of viable cells present. These enzymes are capable of reducing the tetrazolium dye MTT 3-(4,5-dimethylthiazol-2-yl)-2, 5-diphenyltetrazolium bromide to its insoluble formazan, which has a purple color. Other closely related tetrazolium dyes including XTT, MTS and the WSTs, are used in conjunction with the intermediate electron acceptor, 1-methoxy phenazine methosulfate (PMS).<sup>[1]</sup> Tetrazolium dye assays can also be used to measure cytotoxicity (loss of viable cells) or cytostatic activity (shift from proliferation to quiescence) of potential medicinal agents and toxic materials. MTT assays are usually done in the dark since the MTT reagent is sensitive to light.

MTT is a yellow tetrazole, is reduced to purple formazan in living cells.<sup>[2]</sup> A solubilization solution (usually either dimethyl sulfoxide, an acidified ethanol solution, or a solution of the [detergent sodium dodecyl sulfate](#) indiluted [hydrochloric acid](#)) is added to dissolve the insoluble purple [formazan](#) product into a colored solution. The absorbance of this colored solution can be quantified by measuring at a certain wavelength (usually

between 500 and 600 nm) by a spectrophotometer. The degree of light absorption depends on the solvent.

#### IV. RESULT AND DISCUSSION

**4.1 FTIR:** The FTIR spectrum was recorded using Jasco 4100 (TOKYO, JAPAN) with IR resolution software. The scanning range was 4000-400  $\text{cm}^{-1}$ . FTIR measurements were obtained on a pure sample of Carbon Nanotubes.

##### I) FTIR of Pure Carbon nanotubes (CNTs)

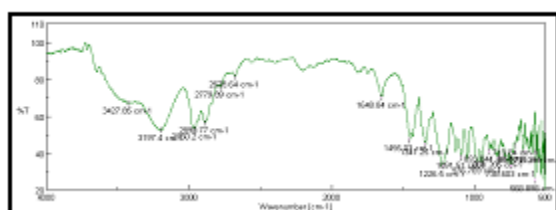


**Figure 1.** FTIR of Pure CNTs

Broad band at 3427  $\text{cm}^{-1}$  and 3197  $\text{cm}^{-1}$  is attributed to presence of O-H groups on the surface of pure CNTs. Peak at 2960  $\text{cm}^{-1}$  and 2890  $\text{cm}^{-1}$  shows the C-H stretching of alkane. The characteristic peak at 1648  $\text{cm}^{-1}$  suggests the presence of carbon residue on the CNTs surface.

The characteristic Peak at 1091  $\text{cm}^{-1}$  shows the C-O stretch of the alkoxy group. [34,37,38]

##### II) FTIR of Oxidized Carbon nanotubes (O-CNTs)

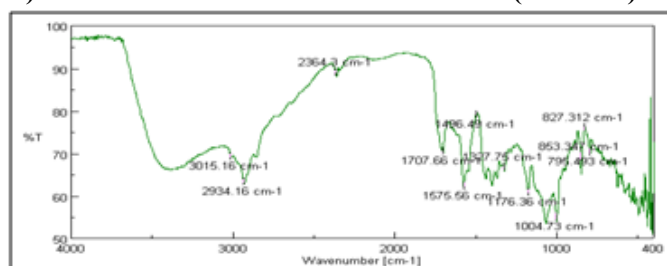


**Figure 2.** FT/IR OF O-CNTs

Oxidised CNTs shows characteristic peak at 3447  $\text{cm}^{-1}$  and 2934  $\text{cm}^{-1}$  due to O-H and C-H stretching of  $\text{CH}_2$  functional groups respectively. The characteristic peak at 1707  $\text{cm}^{-1}$  was found for asymmetric stretching of C=O bond due to COOH group. The characteristic peak at 1176  $\text{cm}^{-1}$  shows C-O stretching of the alkoxy group. [38,43]

##### III) FTIR of Amide Functionalized Carbon nanotubes (CNTs)

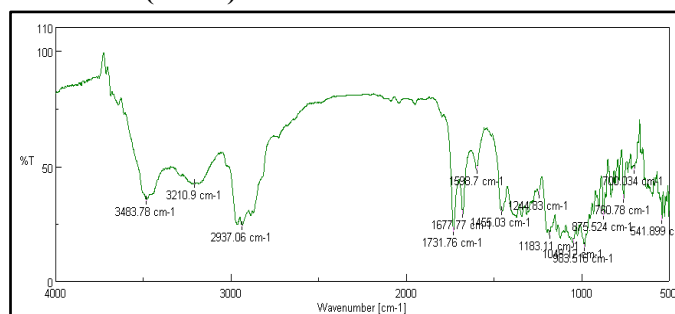


**Figure 3.** FT/IR of Amide Functionalized-CNTs

Shows Disappearance of the band at 1707  $\text{cm}^{-1}$  & corresponding appearance of band with lower frequency 1677  $\text{cm}^{-1}$  assigned to the amide carbonyl (C=O) stretch.

In addition, the presence of the band at 1598  $\text{cm}^{-1}$  and 1183  $\text{cm}^{-1}$ , corresponding to (N-H) in plane and (C-N) bond stretching respectively, this confirms that presence of amide functional group. The characteristic peak at 1048  $\text{cm}^{-1}$  was due to C-O stretching of the ether linkage. [38,9,6]

##### IV) FTIR of Cyclophosphamide loaded on AMIDE F-CNTS

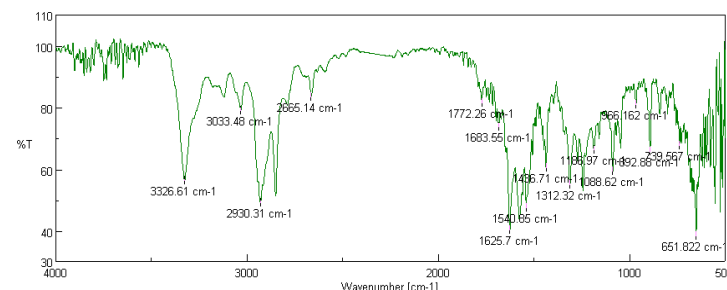


**Figure 4.** FTIR of FA-EDA-MWCNTs/CP Conjugate

Cyclophosphamide loaded on Amide F-MWCNTs shows the characteristics peak at 3303  $\text{cm}^{-1}$  which is indicates that O-H stretching. The characteristic peak at 3326  $\text{cm}^{-1}$  shows the N-H stretching that mask the N-H stretching peak. The characteristic peak at 2930  $\text{cm}^{-1}$  shows the C-H stretching. peak at 1683  $\text{cm}^{-1}$  shows the C=O stretch of intra hydrogen bonded quinone, The characteristic peak at 1088  $\text{cm}^{-1}$  shows the C-O bending. [37,44]

## 2. U.V.Spectroscopy

UV Visible Spectrophotometer (Jasco V630) was used for the characterization purpose. Samples were scanned over the range of 200-400nm.

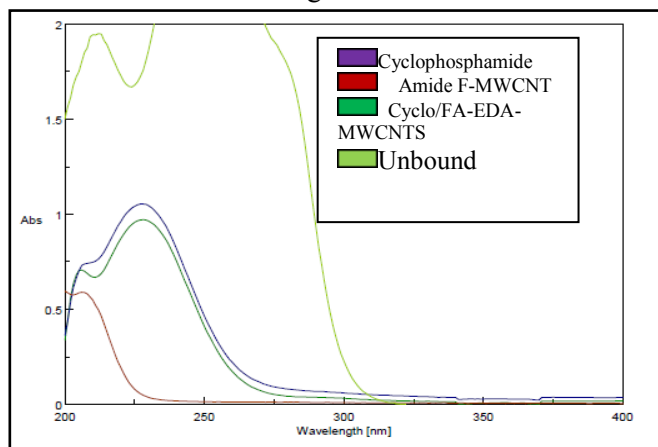


**Figure 5.** U.V. visible Spectroscopy

UV-visible spectrometry was used to characterize the FA-EDA-MWCNTs/CP conjugates (Figure No-5). The U.V visible spectrum of pure Cyclophosphamide exhibit the typical absorption band of in the range of 216,218,226 nm which can be also observed in conjugated MWCNTs-/CP (FA-EDA-MWCNTs/CP). This confirmed the successful attachment of drug molecule to the surface of amide Functionalized-Multi-Walled Carbon Nanotubes (F-MWCNTs). For further confirmation, we observed the U.V visible spectrum of the supernatant of the centrifuged solution which represents the unbound CP. As results, no absorption band was observed in the 216,218 and 226 nm range. U.V visible spectroscopy studies showed that CP molecule successfully loaded on the surface of amide functionalized carbon nanotubes.

## 3) N.M.R.

### 3.1 <sup>1</sup>H-NMR OF OxidizedMWCNTs:-

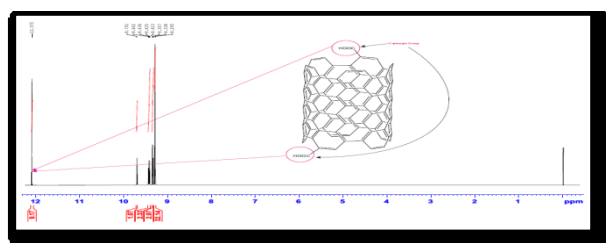


**Figure 6.** <sup>1</sup>H-NMR Spectrum of Oxidized MWCNTs

**Table 1.** Interpretation of <sup>1</sup>H-NMR Spectrum of Oxidized MWCNTs

( $\delta$ ) ppm	Splitting	Assign	Functional Group
12.07	S	-COOH	Carboxylic acid
9.70	S	-CH	Aromatic
9.43	Dd	-CH	Aromatic
9.33	M	- CH	Aromatic
9.293	S	- CH	Aromatic

The <sup>1</sup>H-NMR Spectrum of Oxidized MWCNTs shows in the (figure 19). The Oxidized MWCNTs shows the chemical shift at 12.073 ppm, which indicates that, the presence of carboxylic acid group on the surface of Oxidized-MWCNTs. The chemical shift between 9.70 to 9.29 ppm which indicates that the presence of aromatic (-CH) group on the surface of Oxidized-MWCNTs.

### 3.2 <sup>1</sup>H-NMR OF Folic Acid-Ethylene Diamine (FA-EDA):-

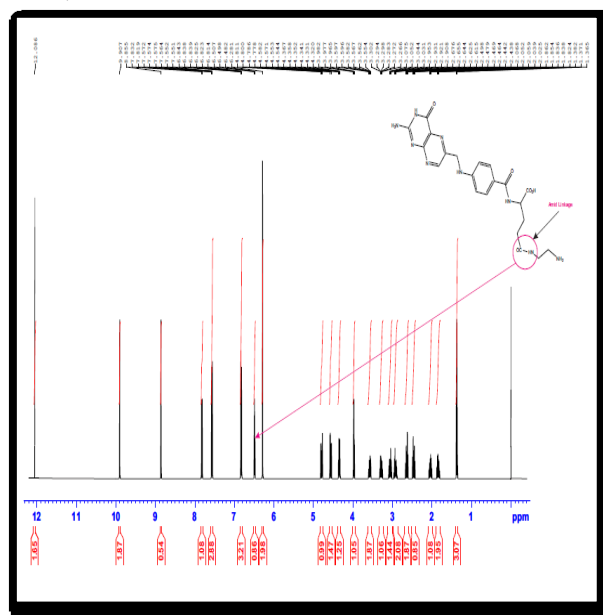


**Figure 7.** <sup>1</sup>H-NMR Spectrum of Folic Acid-Ethylene Diamine (FA-EDA)

**Table 2.** Interpretation of <sup>1</sup>H-NMR Spectrum of Folic Acid-Ethylene Diamine (FA-EDA):-

( $\delta$ ) ppm	Splitting	No. of Proton	Assign	Functional Group
12.08	s	1	- COOH	Carboxylic acid
9.89	s	1	-NH	Pteridine ring
8.88	s	1	-CH	

7.59	m	1	-CH	Para-amino- benzoic acid
6.88	m	1	-CH	
3.97	t	1	-NH	
6.498	t	1	- CONH	Amide

The characteristic signal of the pteridine ring proton of Folic Acid (FA) shows the chemical shift at 9.89 & 8.88 and aromatic & amine protons of the P-Amino-Benzoic Acid (PABA) of Folic Acid (FA) shows the chemical shift at 7.59, 6.88 & 3.97 ppm<sup>[20]</sup> (Figure 7)

The characteristic signal of the formation of -CONH (amide bond) between folic acid and ethylene di-amine conjugate shows the chemical shift at 6.498 ppm which indicates that folic acid successfully conjugated with ethylene di-amine.

### 3.3 <sup>1</sup>H-NMR OF Amide F-MWCNTs (FA-EDA-Oxi MWCNTs):

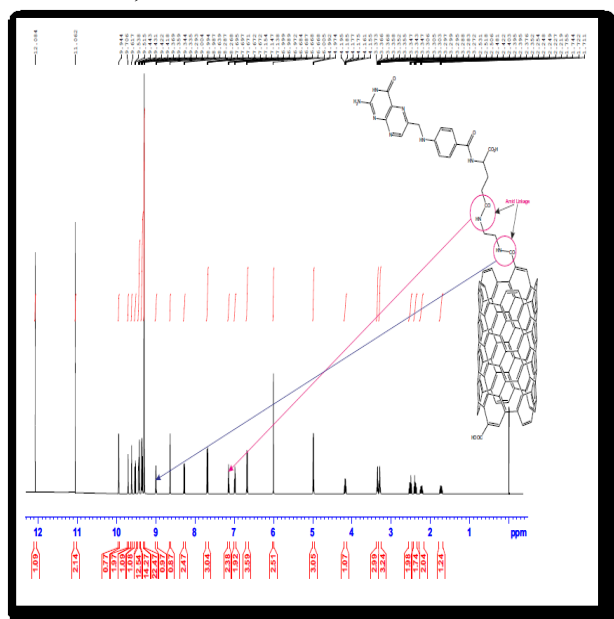


**Figure 8.** <sup>1</sup>H-NMR Spectrum of Amide F-MWCNTs (FA-EDA-Oxi MWCNTs)

**Table 3.** Interpretation of <sup>1</sup>H-NMR Spectrum of Amide F-MWCNTs (FA-EDA-Oxi MWCNTs)

( $\delta$ ) ppm	Splitting	No. of Proton	Assign	Functional Group
12.08	s	1H	- COOH	Carboxylic acid
11.06	s	1H	- COOH	
9.94	S	1H	-NH	Pteridine ring

6.00	s	2H	-NH <sub>2</sub>	Para-amino- benzoic acid
8.63	s	1H	-CH	
4.98	d	2H	-CH <sub>2</sub>	
7.68	m	1H	-CH	
6.67	m	1H	-CH	Para-amino- benzoic acid
6.98	t	1H	-NH	
8.994	t	1H	- CONH	Amide
7.154	T	1H	- CONH	

The <sup>1</sup>H NMR spectrum of the FA-EDA-MWCNTs conjugate are shown in the (figure 8).

The chemical shift at 12.08 ppm and 11.06 ppm which indicates that the presence of carboxylic acid group on the surface of FA-EDA-MWCNTs conjugate.

The characteristic signal of the pteridine ring proton of Folic Acid (FA) shows the chemical shift at 9.94, 8.63, 6.00 & 4.98 ppm and aromatic & amine protons of the P-Amino-Benzoic Acid (PABA) of Folic Acid (FA) shows the chemical shift at 7.68, 6.98 & 6.67 ppm<sup>[20]</sup>

The characteristic signal of the formation of two -CONH (amide bond) between folic acid and ethylene di-amine conjugate shows the chemical shift at 7.154 ppm and folic acid-ethylene diamine (FDA-EDA) with oxidized MWCNTs shows the chemical shift at 8.994 ppm which indicates that FA-EDA conjugate successfully conjugated with oxidized MWCNTs.

### 4.SEM

The morphology of the pure MWCNTs & Cyclophosphamide loaded on amide functionalized MWCNTs were examined by SEM.(Figure no: 9 and 10)

#### 4.1. SEM of Pure MWCNTs:

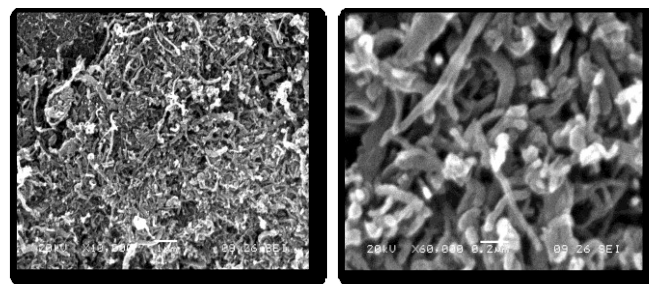


**Figure 9.** SEM Images of CNTs

## 4.2. SEM of CNTs/Cyclophosphamide:

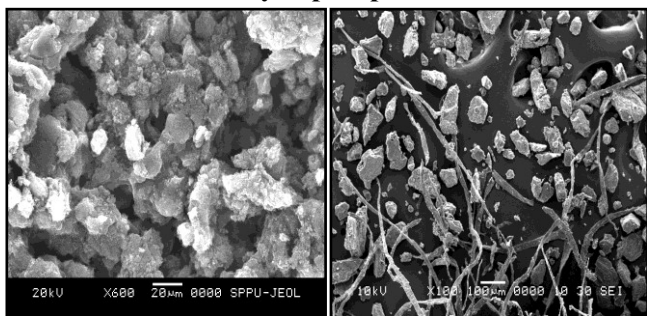


**Figure 10.** SEM of CNTs/Cyclophosphamide

SEM images shows that the change in the morphology between SEM image of Pure MWCNTs & Loaded MWCNTs/CP. The structure of conjugation can be identified, it shows that clear contrast between the SEM image of Pure MWCNTs & MWCNTs loaded with CP. The SEM image of Pure MWCNTs clearly shows that the CNTs are tubular in shape with open ends and in nanometric size range. Where as after loading process of drug with F-MWCNTs the image obtained was not very clear, the size and shape of tubular CNTs is reduced due to the chemical modification of MWCNTs i.e. loading proces.<sup>[39,21]</sup>

## V. ZETA POTENTIAL

ZP is the useful parameter to predict the physical stability. The higher the electrostatic repulsion between the particles the greater is the stability. ZP value more than +20mV or less than -20mV predicts good physical stability.

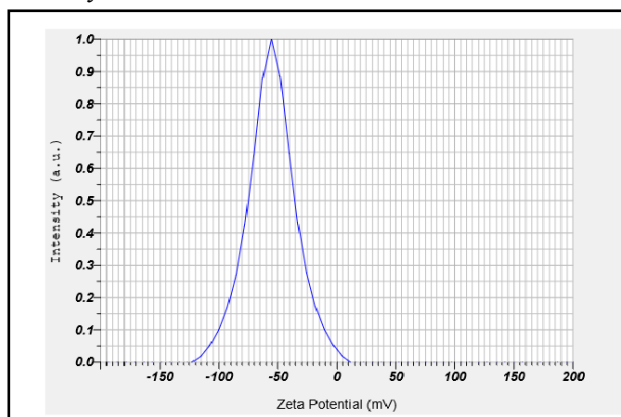


**Figure 11.** Zeta Potential of Pure CNTs

MWCNTs depicted the slightly negative zeta potential (-55.3mV), which could be due to the generation of acidic functional groups during the oxidation process. On increasing the pH the carboxylic acid group becomes more deprotonated leading to the shift of zeta potential

towards negative side. The free COOH group was ionized at alkaline pH & thus negative zeta potential was observed.

## 5.1 Zeta potential of FA-EDA-MWCNTs/CP:

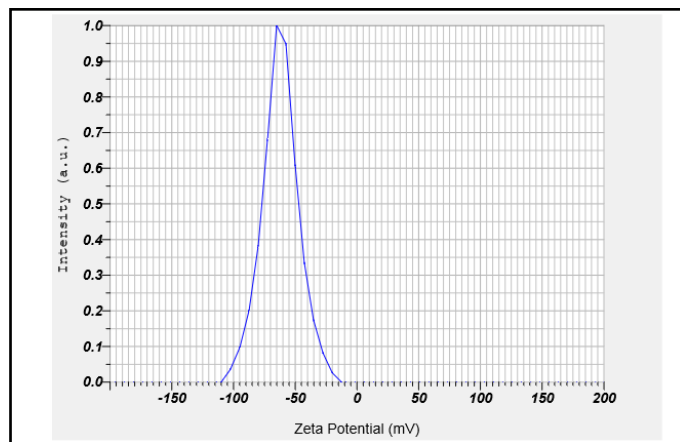


**Figure 12.** Zeta Potential OfFA-EDA-MWCNTs/CP

The zeta potential of FA-EDA-MWCNTs/CP nano-conjugates was found to be (-61.31 mV) (Figure no 25) as that of oxidized-MWCNTs was found to be (-55.3 mV)(Figure no 12). FA-EDA-MWCNTs/Cyclo nano-conjugates shows negative zeta potential value due to the availability of ionisable groups on the FA-EDA-MWCNTs/Cyclonano-conjugates. These significant changes in zeta potential suggest the loading of Cyclophosphamide molecule on the surface of F-MWCNTs. loading of cationic CP molecules on FA decorated MWCNTs shows the changes in zeta potential. Value reflected the successful surface modification of the MWCNTs<sup>[39,8]</sup>

## VI. XRD

Powder X-Ray Diffraction (P-XRD) measurement of pure Cyclophosphamide and Cyclophosphamide loaded with functionalized MWCNTs was performed by using Philips (PW 3710) Expert Pro MPD Diffractometer (PAN Analytical Inc, Germany) with resolution of 0.001 Å°.

## VII. DSC

### 7.1D.S.C. OF PURE DRUG (Cyclophosphamide):

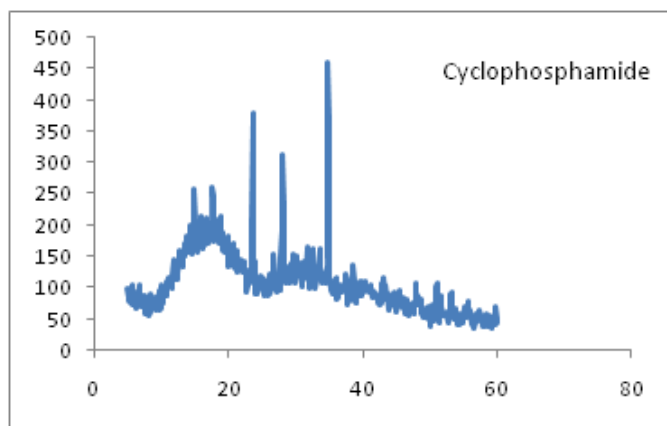


Figure 13. PXRD of Pure Drug

X.R.D analysis of pure Cyclophosphamide shows the peak position in the (Figure No- 13). Cyclophosphamide shows the strong sharp diffraction peak at  $2\theta$  angle  $35.9^\circ$ ,  $23.7^\circ$ ,  $16.7^\circ$ . X.R.D analysis indicates that no. of sharp diffraction peaks was found; hence structure of CP is crystalline in nature.

### 6.1XRD of Loaded CNTs/CP:-

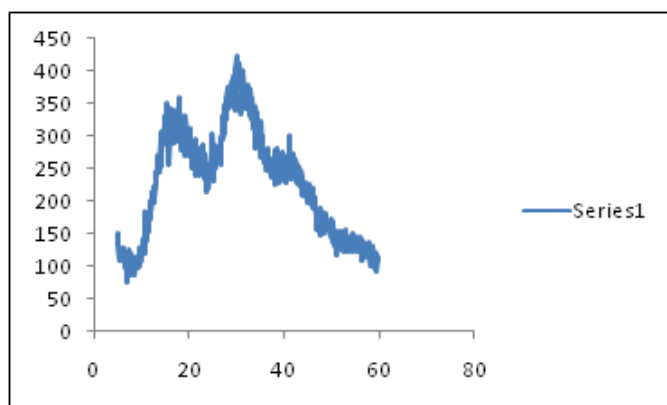


Figure 14. PXRD of Cyclophosphamide loaded MWCNTs

XRD analysis of cyclophosphamide loaded with F-MWCNTs shows the peak in above (figure 14). Cyclophosphamide loaded with F-MWCNTs broad diffraction peak at  $2\theta$  angle  $18.8, 21.5$ , peaks were found hence the drug converted into amorphous form, which implies that the drug is dispersed at a molecular level in the MWCNTs surface<sup>(37,45)</sup>.

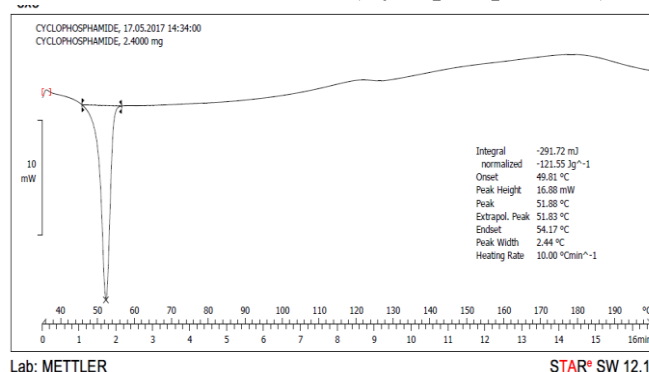


Figure 15. DSC of Pure Cyclophosphamide

The melting point of pure cyclophosphamide was  $49-53^\circ\text{C}$  are reported in literature. DSC study shows that sharp endothermic peak of Cyclophosphamide was at  $51.88^\circ\text{C}$  observed.(Figure No-15). This is corresponding with the M.P of pure Cyclophosphamide.

### 7.2 D.S.C. OF loaded CNTs-DRUG (Cyclophosphamide):

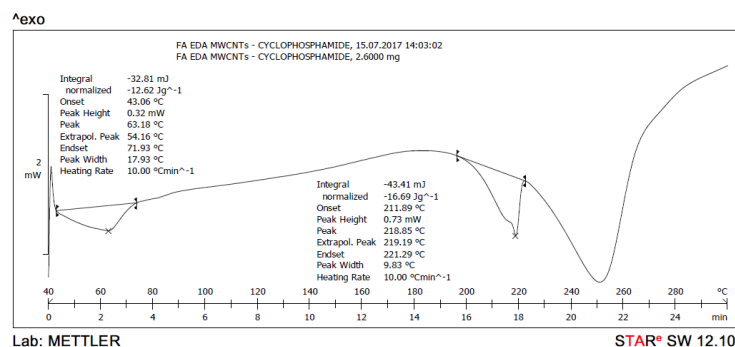


Figure 16. DSC of CNTs-Cyclophosphamide

The DSC graph of loaded MWCNTs cyclophosphamide shows that broad endothermic peak at  $63.18^\circ\text{C}$  was observed which is slight near to the M.P. of pure cyclophosphamide which indicates that small amount of drug is present in the (FA-EDA-MWCNTs/CP) conjugate as shown in Table as below. Two more peaks also present in the graph describe the M.P. of various elements present in the conjugate. The broad peak at  $218.85^\circ\text{C}$  is due to conjugate that is presence of MWCNTs.

**Table 4. Melting Point**

Name	Melting point	
	Observed	Reported
Cyclophosphamide	51.88 <sup>o</sup> C	49-53 <sup>o</sup> C
Cyclophosphamide/MWCNTs	63.18 <sup>o</sup> C	-

**VIII. PARTICLE SIZE ANALYSIS**

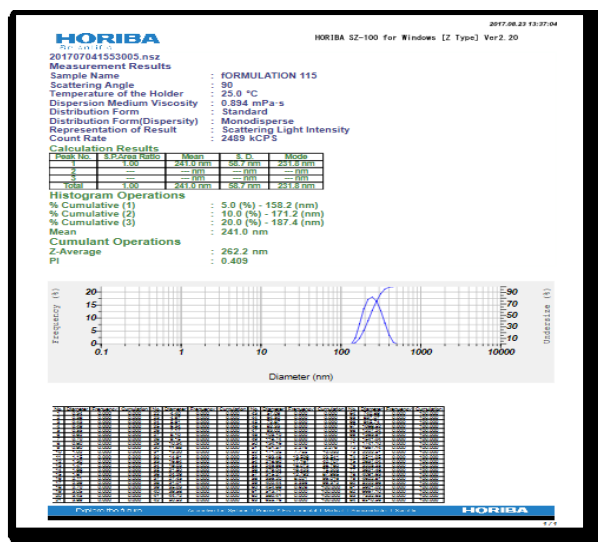


**Figure 17. Particle size of Pure MWCNTs**

The mean particle size of pure MWCNTs was found to be 262 nm (Figure No-17). Lesser the particle size, more is its solubility into the solution. Higher is the solubility, higher is the rate of dissolution. Due to small particle size, they are able to fit into the solvent pockets.

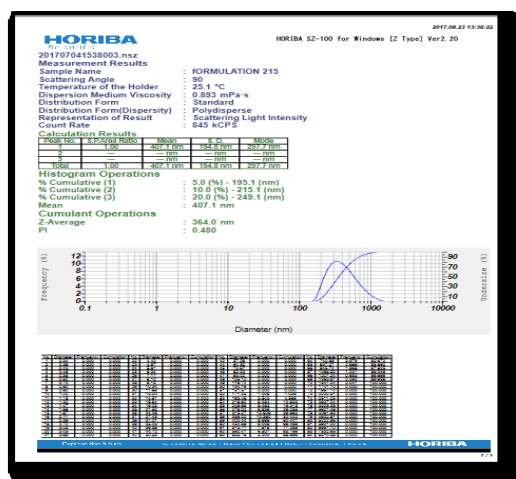


**Figure 18. Particle Size of Cyclophosphamide loaded with F- CNTs**

Particle size increases on loading of drug on the surface of F-MWCNTs. It was found that particle size was increased on loading of the drug which was found to be 407 nm and that of pure MWCNTs was to be 262 nm. Increase in particle size confirms drug has been loaded on the surface of pure MWCNTs.

**IX. POLY DISPERSIVE INDEX (PDI)**

It is measure of distribution of molecular mass in a given polymer sample which indicates the distribution of individual molecular masses in the polymeric solvent. Monodisperse sample have lower PDI value, where higher value of PDI indicates wider particle size distribution.

**Table 5. Polydispersive Index**

PDI	Type of dispersion
0-0.05	Monodispersion
0.05-0.08	Nearly monodisperse
0.08-0.7	Mid-range polydispersity
>0.7	Very polydispersity

PDI of pure MWCNTs and F.A.-EDA-MWCNTs/cyclo nano conjugates was found to be less than 1. Hence the particle size distribution was uniform. The PDI of pure MWCNTs was found to be 0.411 which is less than 0.7 indicating that sample is polydisperse. The PDI of F.A.-EDA-MWCNTs/cyclo nano conjugates was found to be 0.572 which is less than 0.7 indicates that particles are polydisperse [19,20]

Therefore PDI value of sample under investigation was well accepted.

**X. IN-VITRO RELEASE STUDIES**

The cumulative in-vitro release of Cyclo from the FA-EDA-MWCNTs/CP formulations was studied at the normal physiological and lysosomal pH for determining the overall pharmaceutical therapeutic efficacy in blood stream and at target site (Fig-19). The pH of the cytosol is neutral to mildly alkaline (7.4-7.8) while lysosomal pH is acidic (4.0-5.5). During the internalization of the FA-EDA-MWCNTs/CP into the target MCF-7 cells, initially the drug has to be released from the nanotube formulations in order to exert its overall therapeutic effect. The in-vitro release behavior of CP from the

surface engineered MWCNTs formulations exhibited bi-phasic pattern that was characterized by an initial faster followed by sustained release. As expected, the release of CP from FA-EDA-MWCNTs/CP nano-conjugate should be pH-dependent because of the pH-dependent  $\pi$ - $\pi$  stacking interaction between CP and MWCNTs. The release profile of CP from the nano-conjugates was explored under two different pH conditions (pH= 5.3 and 7.4), which represent the acidic microenvironment and physiological environment respectively. It can be seen that at the same point, the CP release rate is faster at pH 5.3 than at pH 7.4. After 48 hr, the cumulative percent CP release was found to be 56.12% at the acidic pH (pH=5.3), while only 39.56 % Cyclo was released at the physiological pH (pH=7.4). The pH-responsive Cyclo release of the FA-EDA-MWCNTs/CP nano-conjugates is beneficial for treating tumor site with slightly acidic pH microenvironment. The initial fast release was attributed to the rapid swelling of CP associated with diffusion and then sustained release of CP was observed due to the limited solubility.

**Table 6.** Diffusion Profile of FA-EDA-MWCNTs/CP

Time (hr)	Sodium acetate buffer pH 5.3 (%)	Phosphate buffer pH 7.4 (%)
2	25.42	16.22
4	27.65	19.45
6	31.26	21.32
8	33.52	22.49
10	34.65	24.79
24	46.23	31.26
48	56.12	39.56
72	58.45	40.39
96	59.23	41.42

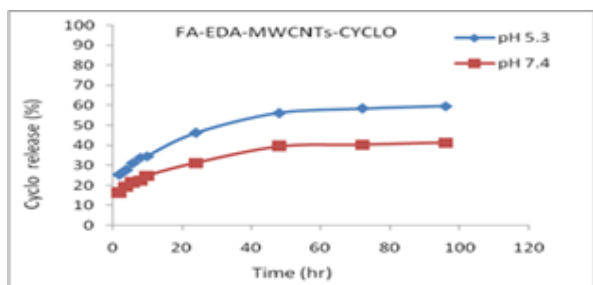


**Figure 19.** Cumulative Cyclo release (%) from FA-EDA-MWCNTs/CP nanoconjugates at  $37 \pm 0.5^\circ\text{C}$  in sodium acetate buffer pH 5.3 and phosphate buffer pH 7.4

## XI. STABILITY STUDIES<sup>44</sup>

Stability study of the nano-conjugates (FA-EDA-MWCNTs/CP) were studied at different conditions of temperature ( $5 \pm 2^\circ\text{C}$ ,  $25 \pm 2^\circ\text{C}$  and  $40 \pm 2^\circ\text{C}$ ), after keeping in dark (amber color bottle) and light (colorless glass vials) and evaluated every week up to 8 weeks. The developed nano-conjugates were found to be most stable in dark at  $5 \pm 2^\circ\text{C}$ . However, on storage in light at  $25 \pm 2^\circ\text{C}$ , slight turbidity was observed, which might be due to aggregation of nanotubes (Table No-7). At  $40 \pm 2^\circ\text{C}$ , the nano-conjugates show the higher turbidity that may be ascribed to the formation of larger aggregates and bundling of nanotubes. In terms of stability profile F-MWCNTs could possibly present themselves as a most stable system due to  $\pi$ - $\pi$  stacking interaction in all temperature ranges and environment required for biological applications. Thus we conclude that the (FA-EDA-MWCNTs/CP) nano-conjugates is more stable in dark at  $5 \pm 2^\circ\text{C}$  than in other  $25 \pm 2^\circ\text{C}$  and  $40 \pm 2^\circ\text{C}$  temperature conditions, and suggesting that the developed nano-conjugate may be suitably stored in amber color bottle or vials at a cool place<sup>[6,20,40,44]</sup>

**Table 7.** Accelerated stability study data for FA-EDA-MWCNTs/CP nano-conjugates:

Stability Parameter	FA-EDA-MWCNTs/CP after 8 weeks					
	Dark ( $^\circ\text{C}$ )			Light ( $^\circ\text{C}$ )		
	$5 \pm 2$	$25 \pm 2$	$40 \pm 2$	$5 \pm 2$	$25 \pm 2$	$40 \pm 2$
		2	2		2	$\pm 2$
Turbidity	-	-	++	+	++	++
Precipitation	-	-	+	-	+	++
Change in color	-	+	+	-	+	++
Crystallization	-	-	+	-	+	+
Change in consistency	-	+	++	-	+	++

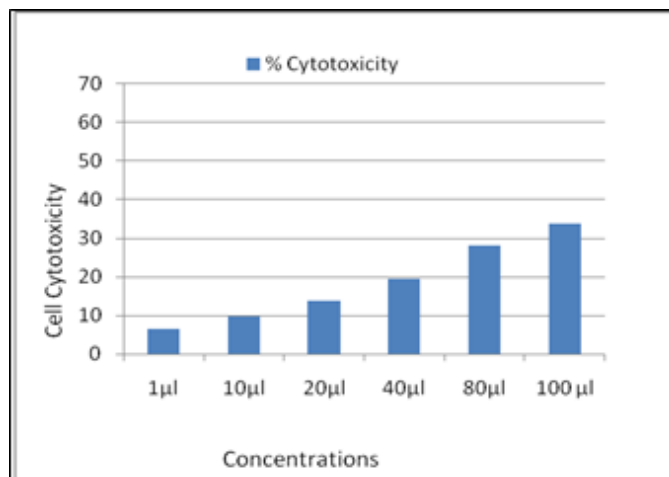
Where, (-) no change; (+) small change; (++) considerable change; (+++) enough change.

## XII. EX-VIVO STUDY: CELL CULTURE STUDY

**METHYL THIAZOLE TETRAZOLIUM (MTT) ASSAY (Cytotoxicity Assay/ Cell Viability Assay)** [43,,51,58].

The MTT assay is a simple, non-radioactive, colorimetry based assay for determining the relative percent cell viability or cell cytotoxicity. The cytotoxicity of Cyclophosphamide conjugated with Functionalized Multi-Walled Carbon Nanotubes (F-MWCNTs) at different micromolar concentrations against MCF-7 (human breast cancer) cells after 24 hr was determined by using MTT cytotoxicity assay. MTT assay clearly revealed that upon increasing the concentration from 1 to 100  $\mu$ M of FA-EDA-MWCNTs/CP nano-conjugates the relative percent cell viability of the cancerous cells was decreased following initial 24 hr treatment due to apoptosis by intercalating CP with DNA. The increased cytotoxic response may possibly be due to caveolae-mediated endocytosis, and specific uptake by cancerous cells causing dose-dependent cytotoxic response. Folate receptors (FRs) are common tumor marker highly over-expressed on the cancerous cells surface that facilitates cellular internalization. Thus, FA-EDA-MWCNTs/CP formulation could efficiently deliver CP to the nucleus of the cell possibly by nanoneedle -transporter or receptor-mediated endocytosis (RME) mechanism.

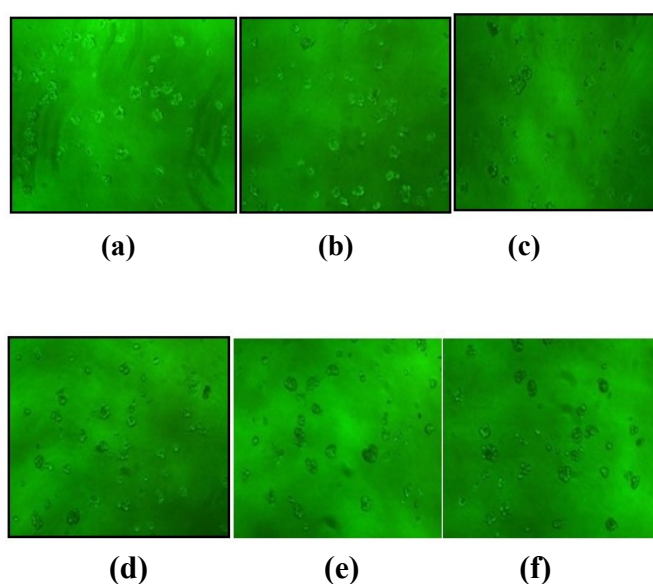
Non-apoptotic cell death (i.e, mitotic catastrophe) is a major response to Cyclophosphamide in human cancer cell lines at the doses and frequencies used in this study. This action of Cyclophosphamide may be partly responsible for their efficacy in treating breast cancers, which are normally resistant to apoptosis. In MCF-7 cells, the drug conjugate FA-EDA-MWCNTs/CP shows the cytotoxicity of 06.46% and 33.88% at 1 $\mu$ g/ml and 100  $\mu$ g/ml respectively (Figure No-26). Reduced apoptosis was observed for drug conjugate on MCF-7 cells, which may be due to the fact that the anti-apoptotic factor Bcl-2 was over expressed and caspase-3 is a major component of the effector phase of the majority of apoptotic signaling pathways, was not expressed. Therefore, the drug conjugate demonstrated less toxicity on MCF-7 cells.

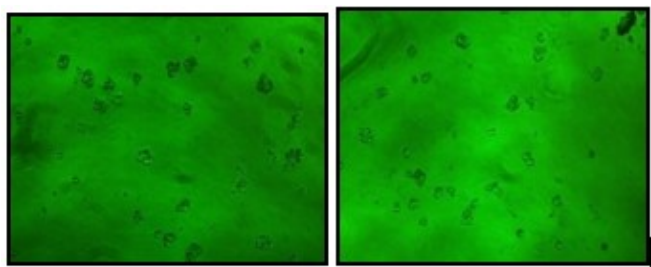


**Figure 20.** Cytotoxicity Study

**Table 8.** % Cell Viability and % Cell Cytotoxicity at different (1 to 100  $\mu$ g/ml) concentrations on MCF-7 cell line.

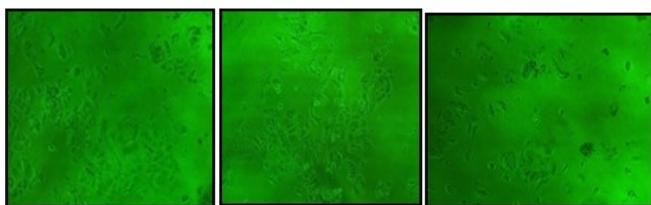
Group	O.D at 492 nm			Mean	% Viability	% Cytotoxicity
Vehicle						
Control	0.055	0.031	0.077	0.054		
Control	0.141	0.124	0.107	0.124		
1 $\mu$ l	0.119	0.107	0.122	0.116	93.54	06.46
10 $\mu$ l	0.103	0.125	0.109	0.112	90.32	09.68
20 $\mu$ l	0.128	0.100	0.093	0.107	86.29	13.71
40 $\mu$ l	0.104	0.100	0.097	0.100	80.64	19.36
80 $\mu$ l	0.093	0.085	0.089	0.089	71.77	28.23
100 $\mu$ l	0.088	0.079	0.083	0.082	66.12	33.88



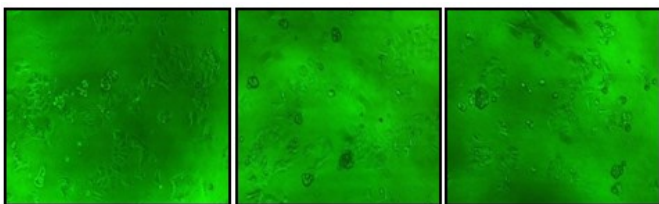


(g) (h)

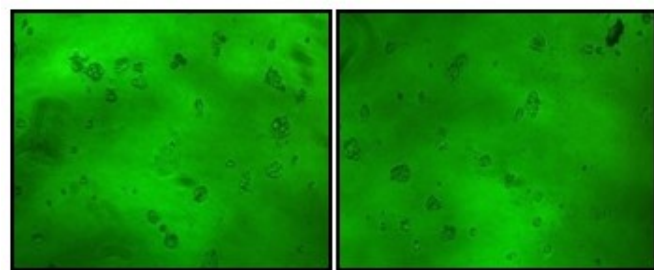
**Figure 21.** Inverted Microscopic Images of MCF-7 Cells at 0 Days (A) Control-1, (B) Control-2, (C) 1  $\mu\text{g/ml}$ , (D) 10  $\mu\text{g/ml}$  (E) 20  $\mu\text{g/ml}$ , (F) 40  $\mu\text{g/ml}$ , (G) 80  $\mu\text{g/ml}$ , (H) 100  $\mu\text{g/ml}$



(a) (b) (c)

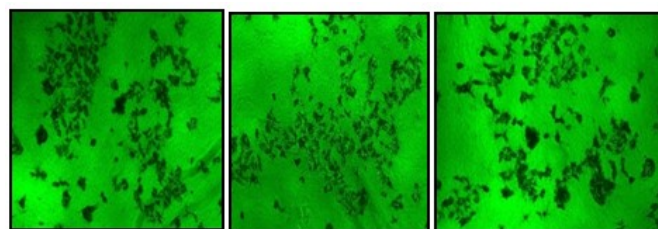


(d) (e) (f)

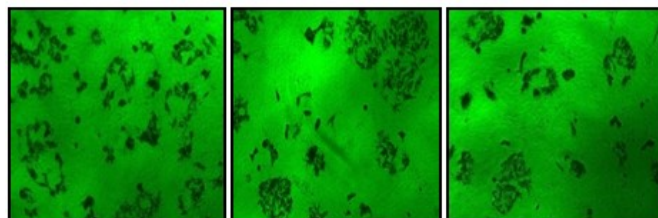


(g) (h)

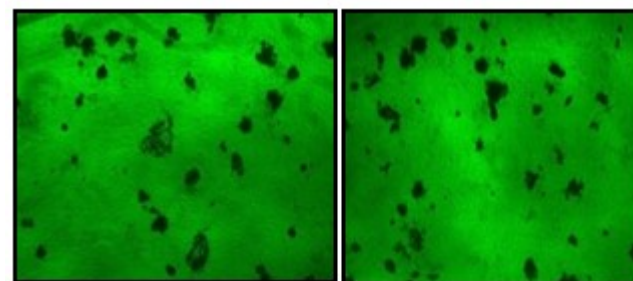
**Figure 22.** Inverted Microscopic Images of MCF-7 Cells treated with CYC/FA-EDA-MWCNTs conjugate after 24 hr (A) Control-1, (B) Control-2, (C) 1  $\mu\text{g/ml}$ , (D) 10  $\mu\text{g/ml}$  (E) 20  $\mu\text{g/ml}$ , (F) 40  $\mu\text{g/ml}$ , (G) 80  $\mu\text{g/ml}$ , (H) 100  $\mu\text{g/ml}$



(a) (b) (c)



(d) (e) (f)



(g) (h)

**Figure 23.** Inverted Microscopic Images of MCF-7 Cells after addition of MTT (A) Control-1, (B) Control-2, (C) 1  $\mu\text{g/ml}$ , (D) 10  $\mu\text{g/ml}$  (E) 20  $\mu\text{g/ml}$ , (F) 40  $\mu\text{g/ml}$ , (G) 80  $\mu\text{g/ml}$ , (H) 100  $\mu\text{g/ml}$

### XIII. CONCLUSION

Efficacy of Cyclophosphamide is lowered due to its significant toxicity, including infusion-related events, such as chills, fever, headache, nausea, vomiting, dose limiting nephrotoxicity. By using CNTs (Loaded with Cyclophosphamide), efficacy of Cyclophosphamide is increased. CNTs are used as carrier for the Delivery of Cyclophosphamide, it acts as needle like work on fungal cell membrane & easily Target the Cancerous cell membrane.

UV-Visible Spectroscopy, NMR & MTT Assay studies shows that Cyclophosphamide successfully loaded to the amide-functionalized Carbon nanotubes.

Results of MTT Assay, clearly shows that the efficacy and Target delivery of Cyclophosphamide is increased which results in less side effects of the drug along with normal cells being unaffected. The covalent linkage of Cyclophosphamide to the CNTs is an approach that may be used to modulate the therapeutic action of the Cyclophosphamide.

From the outcomes of our present research studies, it can be concluded that the CP loaded on surface of amide f-MWCNTs shows the better in-vitro, ex-vivo efficacy as compared to other nano-carriers and sustained release profile especially at acidic micro-environments corresponding to conditions existing at cancerous tissues or sites. In-vitro release studies about 59.23% of CP in FA-EDA-MWCNTs/CP conjugate was release at pH 5.3 suggested that CP release pattern exhibited linear release profile characterized by relatively initial faster release followed by sustained or slower release in the later period.

#### XIV. REFERENCES

- [1]. Mehra N.K, and Jain N.K,"Development, characterization and cancer targeting potential of surface engineered carbon nanotubes", (Journal of Drug Targeting, 3 July 2013, 745-758)
- [2]. Vaibhav Rastogi, Pragya Yadav , Shiv Shankar Bhattacharya, Arun Kumar Mishra, Navneet Verma and jayanta Kumar Pandit,"Carbon Nanotubes: An Emerging Drug Carrier for Targeting Cancer Cells", ( Journal of drug delivery Volume 20141-23)
- [3]. H.Qui,J.Yang," Structure and Properties of Carbon Nanotubes", (Elsevier Publication,2017,47-66)
- [4]. Swatantra Kumar Singh Kushwaha,Saurav Ghoshal,Awani Kumar Rai,Satyawan Singh,"Carbon Nanotubes As A Novel Drug Delivery System For Anticancer therapy: A Review"(Brazalian journal Of Pharmaceutical Sciences,4 Oct,2013,630-642)
- [5]. Rajashree Hirlekar,Manoh Yamagar,Harshal Garse, Mohit Vij,Vilasrao kadam, Carbon Nanotubes And It's Application: A Review (2009); 17-27
- [6]. Neelesh Kumar Mehra and N.K.Jain,"Cancer targeting propensity of folate conjugated surface engineered Multi-Walled Carbon Nanotubes", (Colloids and Surfaces B: Biointerfaces, 27 April 2015)44
- [7]. Maurizio Prato, Kostas Kostarelos and Alberto Bianco, "Functionalized Carbon Nanotubes in Drug Design and Discovery"(Accounts Of Chemical Research,Jan,2008,60-68)
- [8]. Mehra N.k , and Jain N.K," Development , Characterization and Cancer Targeting Potential of Surface Engineered CNTs"(Journal Of Drug Targeting ,3 July 2013,745-758)
- [9]. "Folic Acid". Drugs.com. American Society of Health-System Pharmacists. 1 January 2010. Retrieved 1 September 2016.
- [10]. Florey Klaus, Abdullah A. Al-Badr, Wozniak Timothy J,"Analytical Profile of Drug Substances", Volume-9, Academic Press An Inprint of Elsevier, 24-28 Oval Road, London 2005.
- [11]. Monagle, J. J. (1962). "Carbodiimides. III. Conversion of Isocyanates to Carbodiimides. Catalyst Studies". *J. Org. Chem.* 27 (11): 3851-3855.
- [12]. Sheehan, John; Cruickshank, Philip; Boshart, Gregory, "A Convenient Synthesis of Water-Soluble Carbodiimides", (1961); *J. Org. Chem.* 26 (7): 2525.
- [13]. Good, Norman E.; Winget, G. Douglas; Winter, Wilhelmina; Connolly, Thomas N.; Izawa, Seikichi; Singh, Raizada M. M. "Hydrogen Ion Buffers for Biological Research", (1966); *Biochemistry* 5 (2): 467-477.
- [14]. "N-Hydroxysuccinimide" (<http://www.sigmaaldrich.com/catalog/search/ProductDetail/FLUKA/56480>). Sigma-Aldrich. <http://www.sigmaaldrich.com/catalog/search/ProductDetail/FLUKA/56480>. Retrieved 2007-07-03.
- [15]. Hans-Jurgen Arpe,"Industrielle Organische Chemie-6", Auflage (2007); Seite 245, Wiley VCH.
- [16]. Nabil Fakhre, Alaadin Naqisshbandi,"Spectrophotometric derivation of Cyclophosphamide", (African Journal of Biotechnology,Nov 2013,6531-6537).
- [17]. "Indian Pharmacopeia" Edition 2010, Volume-II, Published by Indian Pharmacopeia Commission, Ghaziabad.
- [18]. Klaus Florey, Jerome I. Bodin, Hans-Georg Leeman,"Analytical Profile of Drug Substances", Volume-9, Academic Press An Inprint of Elsevier, 24-28 Oval Road, London 2005.
- [19]. Neelesh Kumar Mehra and N.K.Jain,"Cancer targeting propensity of folate conjugated surface engineered Multi-Walled Carbon Nanotubes", (Colloids and Surfaces B: Biointerfaces, 27 April 2015)44
- [20]. Neelesh Kumar Mehra, and Narendra Kumar Jain,"One platform comparison of Estrone and Folic acid anchored surface engineered MWCNTs for Doxorubicin delivery", (Molecular Pharmaceutics, ACS Publications Washington DC, 17 Dec 2014)43

- [21]. Sharma Sonam, Neelesh Kumar Mehra, Keerti Jain, and Narendra Kumar Jain, "Effect of functionalization on drug delivery potential of carbon nanotubes" *Artificial cells, Nanomedicine, and Biotechnology* 44, no. 8 (2016): 1851-1860.
- [22]. S.K. Smart, A.I. Cassady, G.Q. Lu, D.J. Martin, "The biocompatibility of carbon nanotubes", S.K. Smart et al. / *Carbon* 44 (2006); 1034-1047
- [23]. T. Ramanathan, Frank T. Fisher, Rodney S. Ruoff, and L. Catherine Brinson, "Apparent Enhanced Solubility of Single-Wall Carbon Nanotubes in a Deuterated Acid Mixture" *Research Letters in Nanotechnology* Volume 2008; 4 pages
- [24]. Vukovic Goran, Aleksandar Marinkovic, Maja Obradovic, Velimir Radmilovic, Miodrag Čolic, Radoslav Aleksic, and Petar S. Uskokovic, "Synthesis, characterization and cytotoxicity of surface amino-functionalized water-dispersible multi-walled carbon nanotubes" *Applied Surface Science* 255, no. 18 (2009): 8067-8075.
- [25]. Joseph Goldstein (2003), "Scanning Electron Microscopy and X-Ray Microanalysis" Springer. ISBN 978-0-306-47292-3. Retrieved 26 May 2012.
- [26]. Huang H, Yuan Q, Shah J.S, Misra R.D.K, "A new family of folate-decorated and carbon nanotubes-mediated drug delivery system: synthesis and drug delivery response" *Adv Drug Deliv. Rev.* 2011, 63, 1332-1339.
- [27]. Vukovic Goran, Aleksandar Marinkovic, Maja Obradovic, Velimir Radmilovic, Miodrag Čolic, Radoslav Aleksic, and Petar S. Uskokovic, "Synthesis, characterization and cytotoxicity of surface amino-functionalized water-dispersible multi-walled carbon nanotubes" *Applied Surface Science* 255, no. 18 (2009): 8067-8075.
- [28]. Shen M, Wang S.H, Shi X, Chen X, Huang Q, Petersen E.J, Pinto R.A, Baker J.R, Weber W.J, "Polyethyleneimine-Mediated Functionalization of Multiwalled Carbon Nanotubes: Synthesis, Characterization, and In Vitro Toxicity Assay", *J. Phys. Chem. C*, 2009, 113, 3150-3156.
- [29]. Zumdahl, Steven S. "Chemical Principles", (2009); 6th Ed. Houghton Mifflin Company. p. A23.
- [30]. "British Pharmacopeia" Edition 2011, Volume-I, Published by British Pharmacopeia Commission, Queen's Road Teddington Middlesex.
- [31]. Good, Norman E.; Winget, G. Douglas; Winter, Wilhelmina; Connolly, Thomas N.; Izawa, Seikichi; Singh, Raizada M. M. "Hydrogen Ion Buffers for Biological Research", (1966); *Biochemistry* 5 (2): 467-477.
- [32]. Son K.H, Hong J.H, Lee J.W, "Carbon nanotubes as cancer therapeutic carriers and mediators" *International Journal of Nanomedicine* 2016, Vol-11, 5163-5185
- [33]. Martel, R. et al. "Ambipolar Electrical Transport in Semiconducting Single-Wall Carbon Nanotubes", (2001); *Physical Review Letters* 87 (25): 256805.
- [34]. Manouchehr Vossoughi, Shiva Gojgini, A. Kazemi, Iran Alemzadeh and Majid Zeinali, "Conjugation of Amphotericin B to Carbon Nanotubes via Amide-Functionalization for Drug Delivery Applications", (Advance online publication: 19 November 2009)
- [35]. V. Datsyuk, M. Kalyva, K. Papagelis, J. Parthenios, D. Tasis, A. Siokou, I. Kallitsis, C. Galiotis, "Chemical oxidation of multiwalled carbon nanotubes", *CARBON* 46(2008); 833-840
- [36]. T. Ramanathan, Frank T. Fisher, Rodney S. Ruoff, and L. Catherine Brinson, "Apparent Enhanced Solubility of Single-Wall Carbon Nanotubes in a Deuterated Acid Mixture" *Research Letters in Nanotechnology* Volume 2008; 4 pages
- [37]. Vukovic Goran, Aleksandar Marinkovic, Maja Obradovic, Velimir Radmilovic, Miodrag Čolic, Radoslav Aleksic, and Petar S. Uskokovic, "Synthesis, characterization and cytotoxicity of surface amino-functionalized water-dispersible multi-walled carbon nanotubes" *Applied Surface Science* 255, no. 18 (2009): 8067-8075.
- [38]. Uttekar. P.S, Kulkarni.A.M, Sable.P.N, Chaudhari.P.D, "Surface modifications of carbon nanotubes with Nystatin for drug delivery applications", (*IJPER: Vol-50, Issue-3, Jul-Sept 2016*).
- [39]. Xueyan Cao, Lei Tao, Shihui Wen, Wenxiu Hou, Xiangyang Shi, "Hyaluronic acid-modified multi-walled carbon nanotubes for targeted delivery of Doxorubicin into cancer cells", (*Carbohydrate Research*, 27 June 2014) 48
- [40]. Neeraj Lodhi, Neelesh Kumar Mehra, and Narendra Kumar Jain, "Development and characterization of Dexamethasone Mesylate anchored on Multi-Walled Carbon Nanotubes", (*Journal of Drug Targeting*, 08 Sept 2012, 21(1):67-76) 46
- [41]. Huang H, Yuan Q, Shah J.S, Misra R.D.K, "A new family of folate-decorated and carbon nanotubes-mediated drug delivery system: synthesis and drug delivery response" *Adv Drug Deliv. Rev.* 2011, 63, 1332-1339.
- [42]. Sharma Sonam, Neelesh Kumar Mehra, Keerti Jain, and Narendra Kumar Jain, "Effect of functionalization on drug delivery potential of

- carbon nanotubes" *Artificial cells, Nanomedicine, and Biotechnology* 44, no. 8 (2016): 1851-1860.
- [43]. Anbarasan B, S. VigneshBabu, K. Elango, B. Shriya, and S. Ramaprabhu, "pH responsive release of doxorubicin to the cancer cells by functionalized multi-walled carbon nanotubes" *Journal of nanoscience and nanotechnology* 15, no. 7 (2015): 4799-4805.
- [44]. ICH Topic Q1A Stability testing Guidelines: stability testing of new drug substances and products, the European agency for the evaluation of medicinal products Human medicines evaluation unit, CPMP/ICH/380/95.
- [45]. Iijima, Sumio; Ichihashi, Toshinari, "Single-shell carbon nanotubes of 1-nm diameter", (1993); *Nature* 363 (6430): 603-605
- [46]. H.Qui, J. Yang, Structure and properties Of Carbon Nanotubes (2017):47-65
- [47]. Flahaut, E.; Bacsá, R; Peigney, A; Laurent, C "Gram-Scale CCVD Synthesis of Double-Walled Carbon Nanotubes". *Chemical Communications* (2003); 1442-1443
- [48]. Rajashree Hirlekar, Manohar Yamagar, Harshal Garse, Mohit Vij, Vilasrao kadam, Carbon Nanotubes And It's Application: A Review (2009); 17-27
- [49]. Kinghong Kwok, Wilson K.S. Chiu. "Growth of carbon nanotubes by open-air laser-induced chemical vapor deposition" *Carbon* 43 (2005); 437-446
- [50]. K. Jurewicz, K. Babel, R. Pietrzak, S. Delpoux, H. Wachowska, "Capacitance properties of multi-walled carbon nanotubes modified by activation and ammoxidation" *Carbon* 44 (2006); 2368-2375
- [51]. Harini Kantamneni, Akhila Gollakota, "carbon Nanotubes Based Systems for targeted drug delivery: A Review" (*International Journal of Engineering Research & Technology*, Feb, 2013, 1-9)
- [52]. Alberto Bianco, Kostas Kostarelos and Maurizio Prato, "Applications of carbon nanotubes in drug delivery, *Current Opinion in Chemical Biology*" (2005); 9:674-679)
- [53]. Wolfgang K. Maser, Ana M. Benito, M. Teresa Martinez, Production of carbon nanotubes: the light approach, *Carbon* 40 (2002); 1685-1695
- [54]. S.K. Smart, A.I. Cassady, G.Q. Lu, D.J. Martin, The biocompatibility of carbon nanotubes, *Carbon* 44 (2006); 1034-1047
- [55]. Jonathan N. Coleman, Umar Khan, Werner J. Blau, Yurii K. Gun'ko, "Small but strong: A review of the mechanical properties of carbon nanotube-polymer composites", *Carbon* 44 (2006); 1624-1652 [52]
- [56]. V. Datsyuka, M. Kalyvaa, K. Papagelis, J. Partheniosa, D. Tasis, A. Siokoua, I. Kallitsisa, c. Galiotis, "Chemical oxidation of multiwalled carbon nanotubes", *CARBON* 46 (2008); 833 - 840